Frontiers of Information Technology & Electronic Engineering
www.jzus.zju.edu.cn; engineering.cae.cn; www.springerlink.com
ISSN 2095-9184 (print); ISSN 2095-9230 (online)
E-mail: jzus@zju.edu.cn

Correspondence:

Planar dual-polarized millimeter-wave shared-aperture array antenna with high band isolation*

Yuyan CAO[1], Zijun GUO[1], Zhangcheng HAO‡[1,2,3]

[1]*State Key Lab of Millimeter Waves, School of Information Science and Engineering, Southeast University, Nanjing 210096, China*

[2]*Frontiers Science Center for Mobile Information Communication and Security, Southeast University, Nanjing 210096, China*

[3]*Purple Mountain Laboratories, Nanjing 211111, China*

E-mail: yuyancao@aa.seu.edu.cn; zjguo@seu.edu.cn; zchao@seu.edu.cn

Received Mar. 27, 2022; Revision accepted May 29, 2022; Crosschecked Sept. 15, 2022

https://doi.org/10.1631/FITEE.2200122

A planar millimeter-wave shared-aperture array antenna is proposed and designed in this paper. By composing the substrate integrated waveguide (SIW) and the stripline, the K-band antenna is embedded inside the Ka-band antenna to achieve a smaller size and a low profile by sharing an aperture. The Ka-band antenna radiates through the parallel slot pairs on the surface of the SIW cavities with horizontal polarization, while the K-band antenna radiates through the butterfly-shaped slots with vertical polarization, which are also designed on the surface. Then the two array antennas can radiate by sharing a common aperture with high isolation. To verify this idea, a prototype of an 8×8 shared-aperture array antenna has been designed with center frequencies of 19 and 30 GHz and fabricated using multilayer printed circuit board (PCB) technology. The measurement results show that the −10 dB impedance bandwidths in the K- and Ka-bands are 7.73% and >20%, and the corresponding isolations are higher than 60 and 44 dB, respectively. The proposed shared-aperture antenna has a small footprint, a low profile, and high isolation, and is a promising candidate to design compact millimeter-wave wireless systems.

1 Introduction

With the urgent need for system miniaturization and high integration, planar shared-aperture antennas have received much attention due to their compact sizes and flexible functions, such as multi-band operation and multi-polarization capability (Smolders et al., 2013; Zhang JD et al., 2016; Tao et al., 2021; Zhou et al., 2021). More importantly, by adopting a shared-aperture array antenna, the aperture utilization can be greatly improved, and the number of antennas in the wireless system can be reduced. Recently, a few techniques have been proposed to develop the shared-aperture antennas with good performance, such as the nested technique (Zhao et al., 2015; Mao et al., 2017a, 2017b), the staggered technique (Naishadham et al., 2013; Mao et al., 2017c), and the stacked technique (Ho and Rebeiz, 2014; Wang et al., 2018; Ferrando-Rocher et al., 2019). As millimeter-wave wireless systems have become popular, millimeter-wave shared-aperture antennas have drawn great attention of researchers (Ho and Rebeiz, 2014; Ding

‡ Corresponding author

* Project supported by the National Natural Science Foundation of China (No. 62131008) and the Fundamental Research Funds for the Central Universities, China (No. 2242022k30003)

ORCID: Yuyan CAO, https://orcid.org/0000-0003-3360-7450; Zijun GUO, https://orcid.org/0000-0001-9139-310X; Zhangcheng HAO, https://orcid.org/0000-0002-1835-7652

and Cheng, 2019; Ferrando-Rocher et al., 2019; Zhang JF et al., 2020). A planar shared-aperture array antenna is highly desired for wireless systems, and can dramatically reduce the system size. However, due to the challenges of both the element and array designs in the millimeter-wave band, only a few planar millimeter-wave shared-aperture array antennas have been reported with good performance in recent years (Cheng et al., 2017; Xu LM et al., 2019; Zhang JF et al., 2019; Guo et al., 2021; Hong et al., 2021).

2 Antenna and array design

2.1 Operating principle of the proposed antenna element

Fig. 1 presents the configuration of the proposed K-/Ka-band orthogonal linear polarization shared-aperture antenna element. It is composed of four Rogers RO4350 substrates (ε_r=3.66 and tan δ=0.004) and two Rogers RO4450F bondply layers (ε_r=3.52 and tan δ=0.004). The thickness of the copper is 0.035 mm, and the corresponding planar layouts are illustrated in Fig. 2 with their detailed geometries.

To achieve a compact profile, the K- and Ka-band antennas are integrated and share the same radiation aperture on the top surface of the SIW cavity. Two types of radiation slots are designed for the two bands, i.e., two rectangular slots and one butterfly-shaped slot. On the top surface of the SIW cavity, two rectangular slots are symmetrically designed with respect to the center with an offset for the Ka-band operation, and they are excited by the SIW cavity from port 1. Besides, the butterfly-shaped slot is designed at the center for K-band operation, excited by a stripline from port 2. Because the butterfly-shaped slot

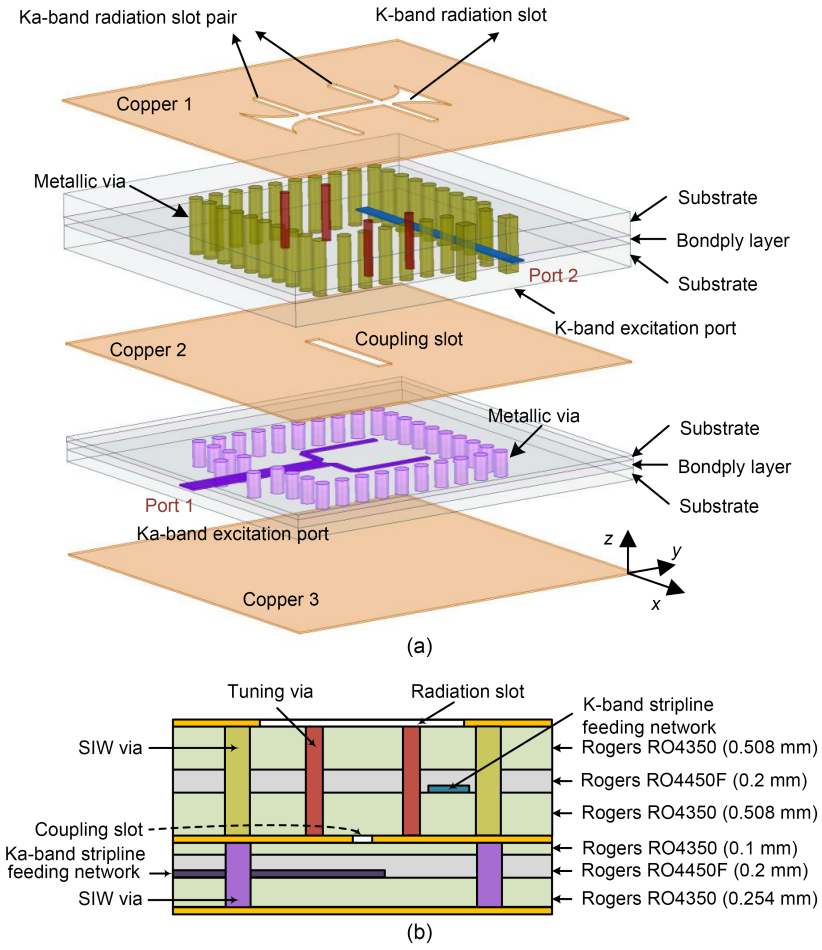

Fig. 1 Configuration of the proposed K-/Ka-band shared-aperture antenna element: (a) three-dimensional view; (b) cross-sectional view

does not cut any surface current of the SIW cavity when the Ka-band element is operated, it has no radiation at the Ka-band. Conversely, when the K-band element is operated, the two rectangular slots function as two parasitic radiation slots with opposite radiation phases. Their radiation fields are canceled, and the main radiation is from only the butterfly-shaped slot. Consequently, the K- and Ka-band element antennas can be simultaneously operated with high isolation and share the same radiation aperture.

2.2 Design of the antenna element

Ka-band antenna is operated with a slotted SIW cavity, which is fed by the stripline from port 1 at lower substrate layers and then coupled through the coupling slot etched on copper 2. Two types of radiation slots, i.e., the Ka-band radiation slot pair and the K-band radiation slot in Fig. 1a, are orthogonally etched on copper 1. The slots in the x direction radiate the y-polarized waves in the Ka-band, while the slot in the y direction radiates the x-polarized waves in the K-band. The coupling slot is designed at the center of the bottom of the SIW cavity, while the two radiating slots are symmetrically distributed at the center of the SIW cavity. The simulated electrical field distribution of the Ka-band element is shown in Fig. 3. Theoretically, the Ka-band SIW cavity can be excited using a straight stripline through the coupling slot. However, because the straight stripline needs to be placed underneath the K-band radiation slot, unwanted

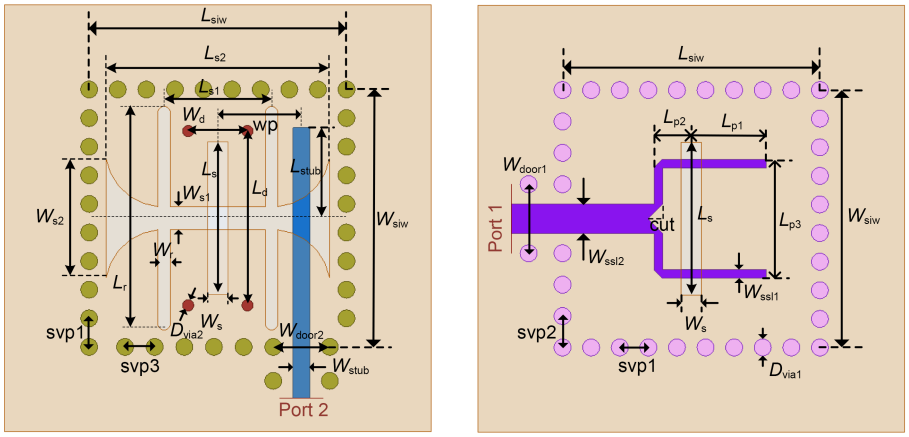

Fig. 2 Geometry of the shared-aperture antenna element: (a) upper substrate layers; (b) lower substrate layers

L_{siw}=W_{siw}=4.55 mm, svp1=0.505 mm, svp2=0.555 mm, svp3=0.52 mm, D_{via1}=0.3 mm, D_{via2}=0.2 mm, W_{ssl1}=0.26 mm, W_{ssl2}=0.52 mm, cut=0.15 mm, L_{p1}=1.5 mm, L_{p2}=0.48 mm, L_{p3}=2.1 mm, L_s=2.7 mm, W_s=0.35 mm, L_r=3.95 mm, W_r=0.22 mm, W_{stub}=0.3 mm, L_{stub}=1.6 mm, wp=1.48 mm, L_{s1}=1.9 mm, L_{s2}=3.95 mm, W_{s1}=0.4 mm, W_{s2}=2.1 mm, L_d=3.08 mm, W_d=1.05 mm, W_{door1}=1.22 mm, W_{door2}=1 mm

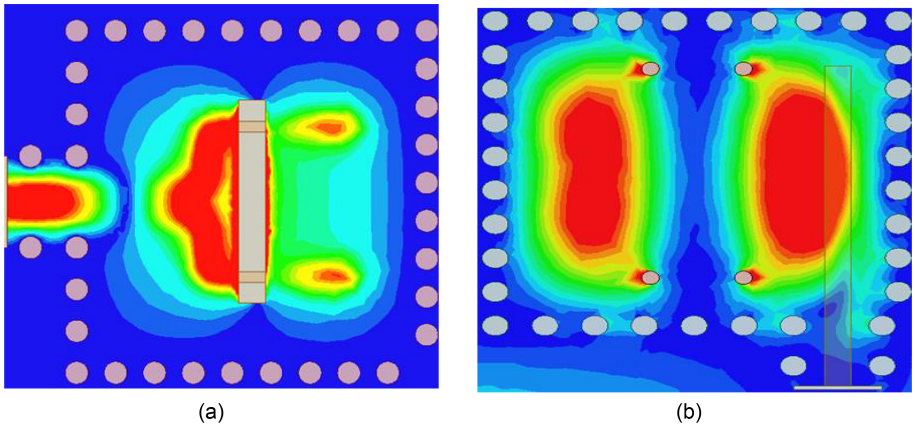

Fig. 3 Simulation of electric field distributions of the Ka-band antenna unit at 30 GHz: (a) lower substrate layers; (b) upper substrate layers

radiations from the feeding structure occur. Moreover, a relatively narrow bandwidth would occur if the Ka-band SIW cavity is fed by the straight stripline (Luo et al., 2008). To overcome these drawbacks, a forked stripline is adopted in the design for the Ka-band SIW cavity excitation. The forked stripline is equivalent to a two-way power divider. Thus, there is a displacement in the x direction between the K-band radiation slot and the forked stripline, as illustrated in Fig. 1a, and the unwanted radiation from the feeding network can be reduced for the Ka-band application. In addition, the forked stripline transforms the single-point excitation of a straight stripline into a double-point excitation with narrow lines. Then, according to the coupling theory, the single resonating peak of the SIW cavity can be slightly split into two resonating peaks. This approach is helpful in extending the operating bandwidth. Ideally, the impedance of the input stripline is expected to be 50 Ω, and the forked striplines have an impedance of 100 Ω. However, because a thin substrate is adopted to achieve a compact size in the design, the 100 Ω impedance stripline has to be designed with an extremely narrow width of around 0.05 mm, which cannot be realized using the PCB process. Consequently, a relatively low impedance stripline, with an impedance of around 30 Ω, has been used as the input/output for the element antenna, and a stripline-to-coplanar waveguide (CPW) transformer is designed for achieving a 50 Ω impedance for the input/output of the array. Accordingly, the forked stripline has an impedance of around 60 Ω. Hence, the initial widths of 0.52 mm and 0.26 mm are adopted for the input and the forked striplines, respectively. The initial size L_{p1} of the forked line is chosen as a quarter-wavelength of the Ka-band. L_{p3} of the forked line is chosen as large as possible to obtain a wide operating bandwidth. In the element design, a space between the end of the coupling slot and the edge of the forked stripline, which is equivalent to the width of the forked line, is initially chosen for the L_{p3}. The initial geometries of the SIW cavity can be determined by classical empirical formulae for the SIW (Zhang Y et al., 2011; Qi et al, 2021), and the initial length of the coupling slot and Ka-band radiation slot pair are chosen as half-wavelength at 30 GHz. Then, the full-wave high-frequency structure simulator (HFSS) is adopted to tune the geometries of the forked line to obtain a wide bandwidth and good in-band impedance matching. The final geometries are shown in Fig. 2.

The K-band antenna is operated with the horizontally placed butterfly-shaped slot etched on copper 1 along the y direction, and excited by the K-band stripline at port 2. In this case, the K-band antenna radiates x-polarized waves and is operated with the transverse electric magnetic (TEM) mode wave, which is coupled from port 2 to the horizontal butterfly-shaped slot through the stripline inside the upper substrate layers. To obtain strong coupling and good in-band impedance matching, four metallic vias are designed around the butterfly-shaped slot. Because the Ka-band slots are etched on copper 1 and are parallel to the K-band feeding stripline, there is almost no coupling between port 2 and the Ka-band radiation slot pair. Initially, the length of the butterfly-shaped slot is designed as half-wavelength at 19 GHz, and then the butterfly-shaped slot is adjusted through L_{s2} and W_{s2} to achieve a broadband −10 dB return loss.

Once the K- and Ka-band antennas are initially designed, they are integrated and tuned using the full-wave HFSS to obtain the final geometries with good performance. As discussed above, because the coupling between the K- and Ka-band excitations is pretty weak, final geometries can be obtained through a fast full-wave optimization process.

Fig. 4a shows the electric field distribution of the K-band element at 19 GHz. When feeding from port 2, the butterfly-shaped slot cuts off the current to generate the x-polarization radiation field. In this case, a very weak coupling can be found from port 2 to port 1. Similarly, the electric field distribution of the Ka-band element at 30 GHz is shown in Fig. 4b, where the antenna is fed from port 1. In this case, most of the quasi-TE_{120} mode field is radiated by the x-direction slot pair. Consequently, a y-polarized radiation wave of the Ka-band element is obtained. Again, a very weak coupling can be found from port 1 to port 2. This is because the two elements only support different operation modes and orthogonal polarizations, and the mode and polarization couplings are small enough to achieve high port isolation.

To support the planar array application, the proposed shared-aperture element is designed with a very compact form. Both its width and length are 4.55 mm,

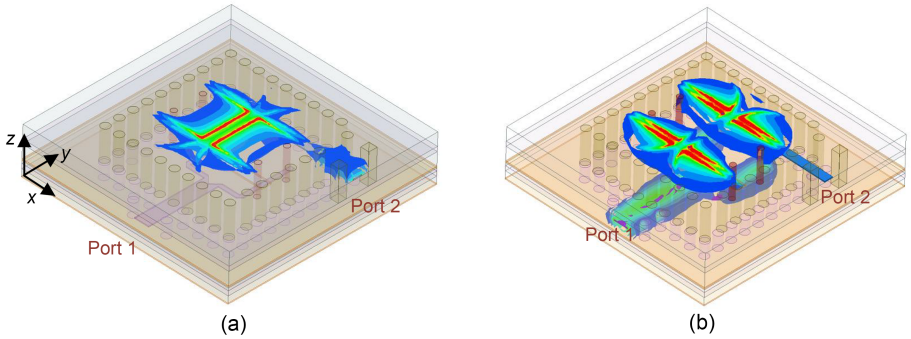

Fig. 4 Electric field distributions of the shared-aperture antenna element at 19 GHz (a) and 30 GHz (b)

i.e., $0.288\lambda_K$ at 19 GHz and $0.455\lambda_{Ka}$ at 30 GHz. The reflection coefficients and the radiation gains of the K- and Ka-band are plotted in Fig. 5. In the K-band, the reflection coefficient of port 2 is lower than −10 dB, from 18.82 GHz to 19.25 GHz (relative bandwidth is 2.26%), and the maximum realized gain is 6.06 dBi. In the Ka-band, the reflection coefficient of port 1 is below −10 dB, from 28.58 GHz to 31.06 GHz (relative bandwidth is 8.32%), and the maximum realized gain is 6.53 dBi. A filtering radiation gain character can be observed in Fig. 5b, which is the result of a two-order filtering coupling of the SIW cavity with a double-excitation strategy using the forked striplines. In addition, because the feeding networks of the K- and Ka-band are designed in different layers with different operating modes and polarizations, the isolation between these ports is relatively high. It can be seen from Fig. 6 that the isolations in the K- and Ka-band are higher than 65 dB and 23 dB, respectively.

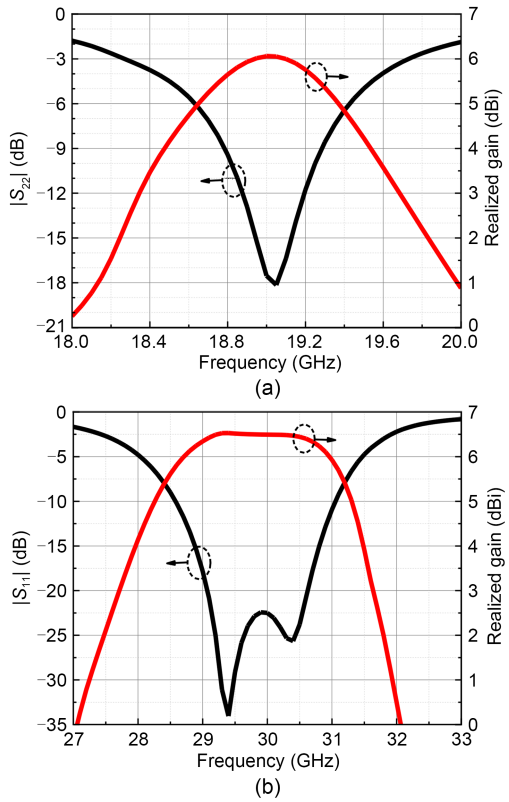

Fig. 5 Simulated reflection coefficients and realized gains of the shared-aperture antenna unit: (a) K-band; (b) Ka-band

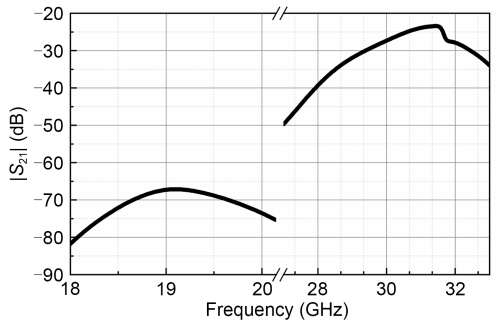

Fig. 6 Simulated isolation between port 1 and port 2 of the antenna element

2.3 Design of the antenna array

The design of an 8×8 array is described in this subsection to demonstrate the planar array application of the proposed shared-aperture element. In the array design, the spacing between the elements is chosen as sp=7.5 mm, i.e., $0.475\lambda_K$ at 19 GHz and $0.75\lambda_{Ka}$ at 30 GHz. This spacing avoids undesired grating lobes of the K- and Ka-band while leaving enough space to design the required feeding networks. Two feeding networks are designed for the K- and Ka-band arrays, respectively, and their layouts and geometries are shown in Fig. 7. Because a very weak coupling exists between the two networks, they

can be designed independently. Both the K- and Ka-band feeding networks are designed in parallel (Xu et al., 2020). Using multiple $\lambda/4$ impedance conversions and T-junction power dividers, the equal amplitude and in-phase output response are realized for 64 ports of each feeding network. Because the stripline feeding networks introduce the parallel plate mode in the operation, metallic vias are added on both sides of the stripline to suppress the parallel plate mode (Mukherjee, 2017). To feed the array antenna with an end launch connector in the experiments, two shielded stripline (SSL)-to-grounded coplanar waveguide (GCPW) transitions are designed for the array (Li et al., 2015). The final three-dimensional configuration of the proposed array antenna is shown in Fig. 8. Fig. 9 shows the simulated insertion loss and reflection coefficients for the designed feeding networks. At the K-band, the reflection coefficient is smaller than −12 dB, and its transmission coefficient is around −20 dB. At the K-band, the reflection coefficient is smaller than −10 dB, and its transmission coefficient is around −21 dB. The insertion losses of the K- and Ka-band feeding networks are around −2 dB and −3 dB, respectively, which is a result of the substrate and metal losses.

3 Experiments and results

The designed 8×8 array prototype was fabricated using the PCB process. Generally, a multilayer process can be adopted to fabricate the full structure with a multiple pressing procedure, but that would be expensive. To reduce the fabrication cost, we individually fabricated the top two substrates and the bottom two substrates using a double-layer PCB process. Then, these two fabricated boards were aligned through an alignment hole with screws. Fig. 10 shows photographs of the fabricated array antenna. The *S*-parameters were measured using the vector network analyzer, and the radiation gain and radiation pattern were measured in a far-field anechoic chamber.

The measured *S*-parameters and realized gains as well as the simulation results are illustrated in Fig. 11. The measured −10 dB impedance bandwidth for the K-band is 7.73% (18.27–19.74 GHz), and the band isolation is higher than 60 dB. The measured maximum realized gain is 18.5 dBi, and the 3 dB gain bandwidth is 9.53% (18.18–20 GHz). In the Ka-band, the measured reflection coefficient is below −10 dB from 27 to 33 GHz, and the bandwidth is higher than 20%. In addition, the band isolation is higher than 44 dB. The measured maximum gain is 20.02 dBi, and the 3 dB gain bandwidth is 10.54% (28.4–31.56 GHz). Generally, the measurement and simulation results agree well, and the small discrepancies are from mainly the alignment and fabrication tolerances.

The typically normalized co- and cross-polarization radiation patterns of the proposed K-/Ka-band shared-aperture antenna are shown in Figs. 12 and 13. Generally, the measured patterns are in good

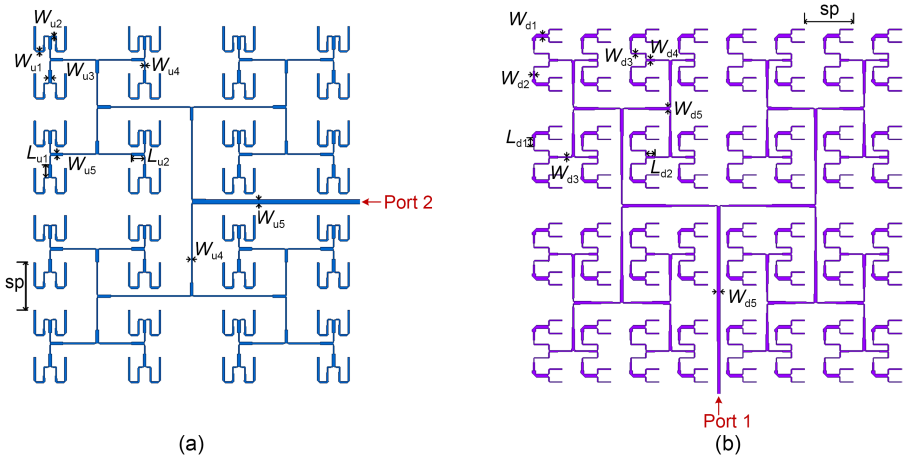

Fig. 7 Layouts of the feeding networks on different layers: (a) K-band feeding network; (b) Ka-band feeding network
W_{u1}=0.3 mm, W_{u2}=W_{u4}=0.18 mm, W_{u3}=0.45 mm, W_{u5}=0.49 mm, W_{d1}=W_{d5}=0.52 mm, W_{d2}=W_{d4}=0.3 mm, W_{d3}=0.15 mm, L_{u1}=2 mm, L_{u2}=1.94 mm, L_{d1}=1.3 mm, L_{d2}=1.29 mm, sp=7.5 mm

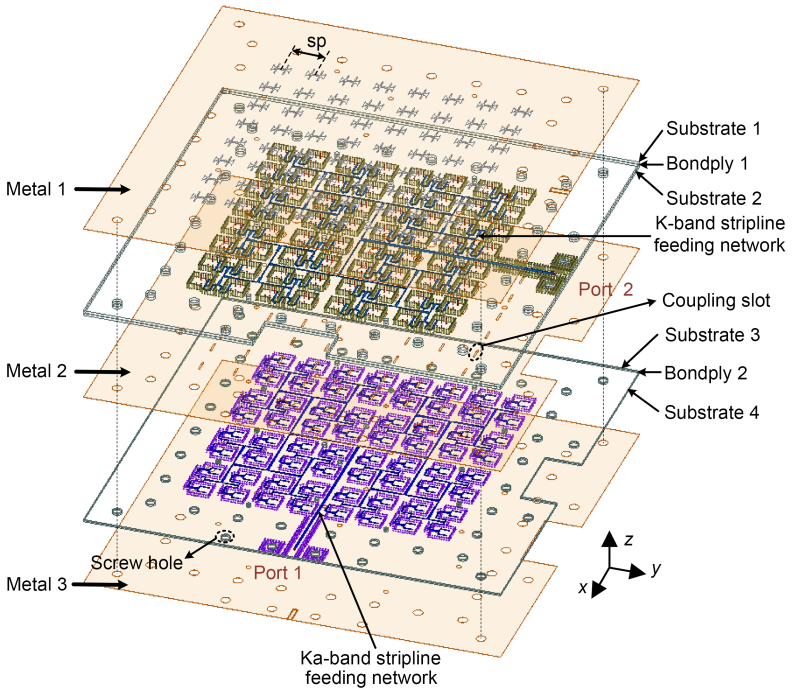

Fig. 8 Three-dimensional configuration of the proposed K-/Ka-band shared-aperture antenna array

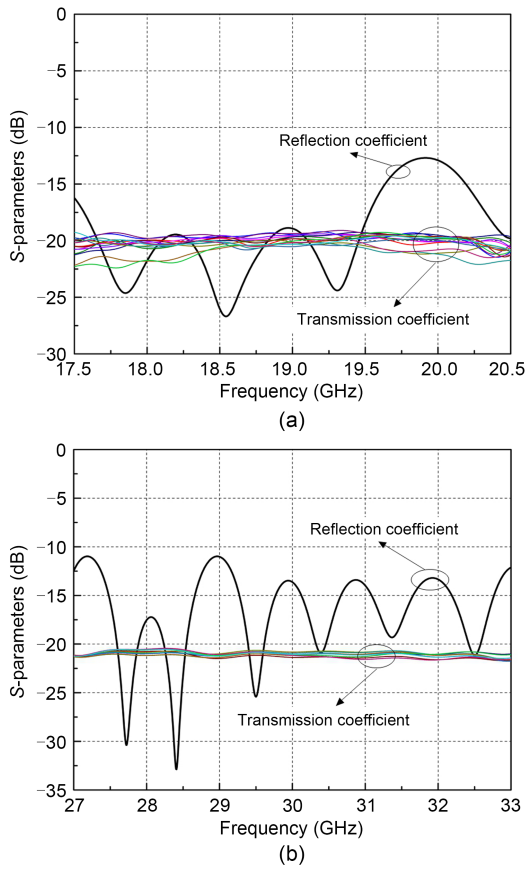

Fig. 9 Simulated insertion losses and reflection coefficients of the designed feeding networks: (a) K-band; (b) Ka-band

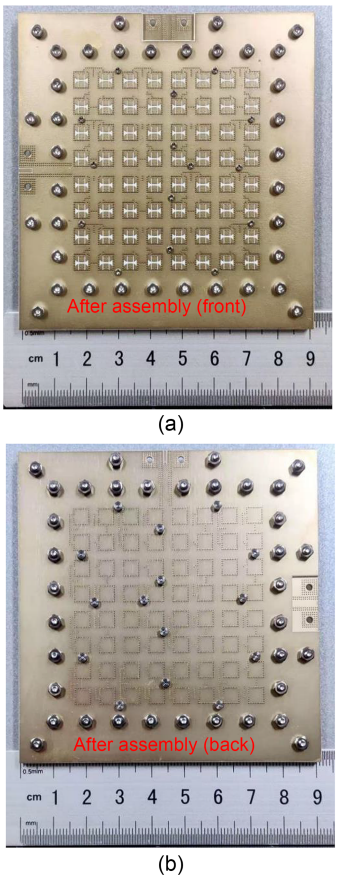

Fig. 10 Photographs of the fabricated shared-aperture array antenna: (a) front view; (b) back view

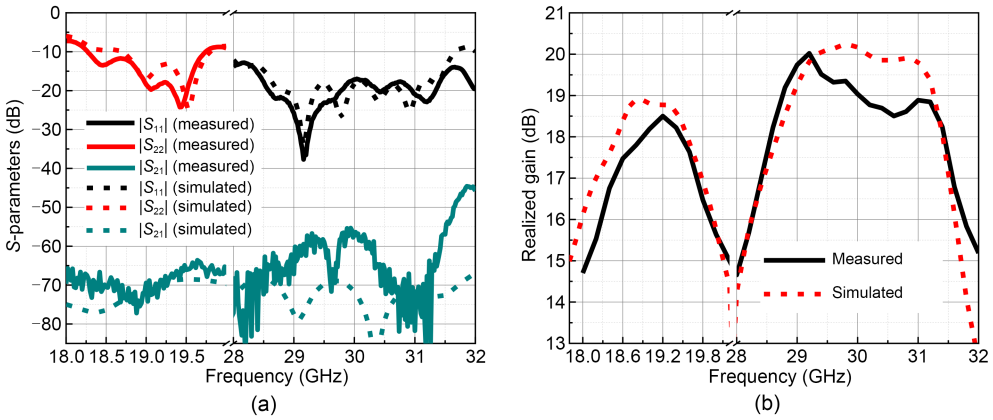

Fig. 11 Simulation and measurement results of the shared-aperture array antenna: (a) magnitude responses for the *S*-parameters; (b) realized gain

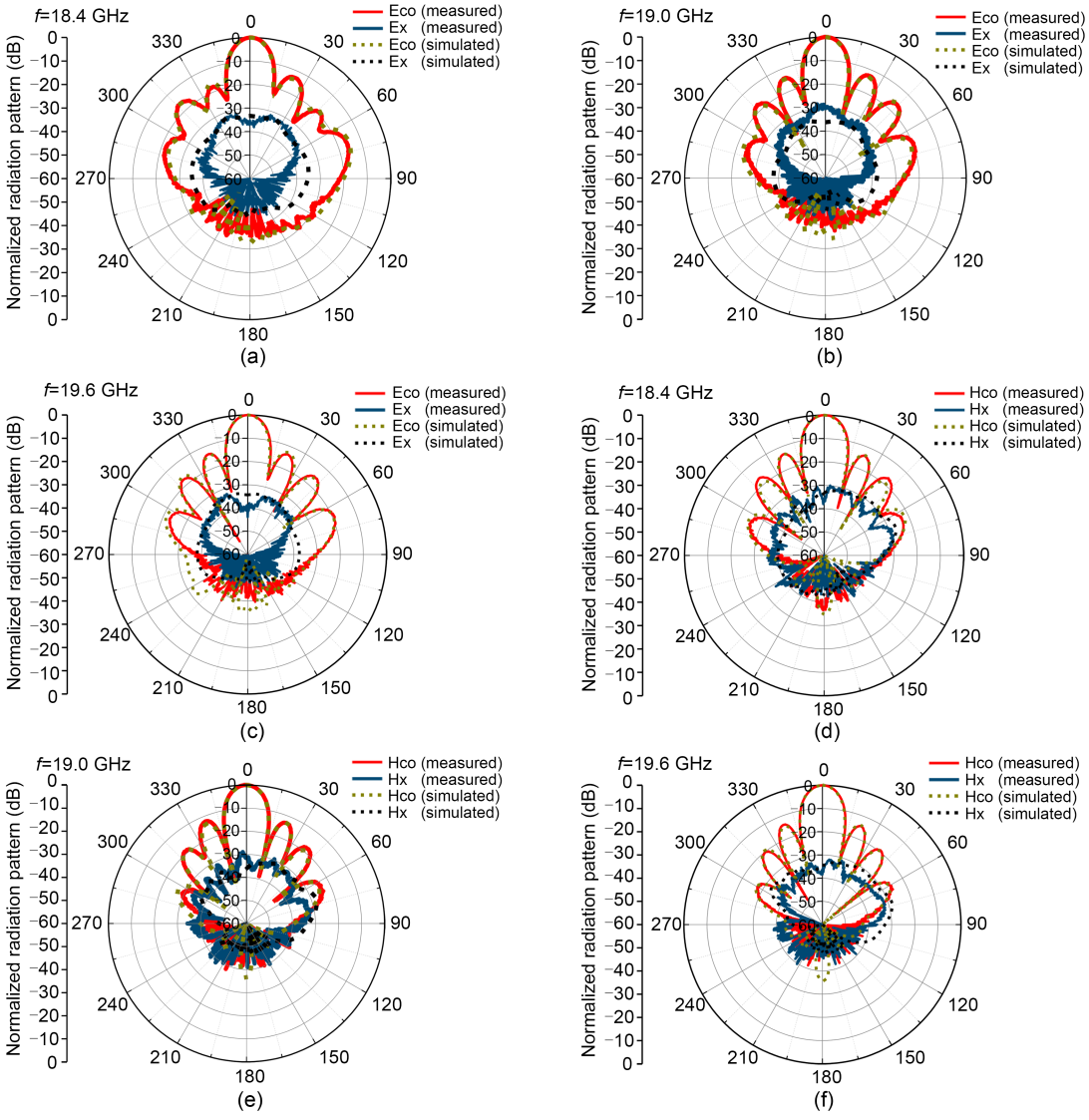

Fig. 12 Simulated and measured normalized radiation patterns of the shared-aperture array antenna at K-band: E-plane (*xoz* plane) at 18.4 GHz (a), 19.0 GHz (b), and 19.6 GHz (c); H-plane (*yoz* plane) at 18.4 GHz (d), 19.0 GHz (e), and 19.6 GHz (f)

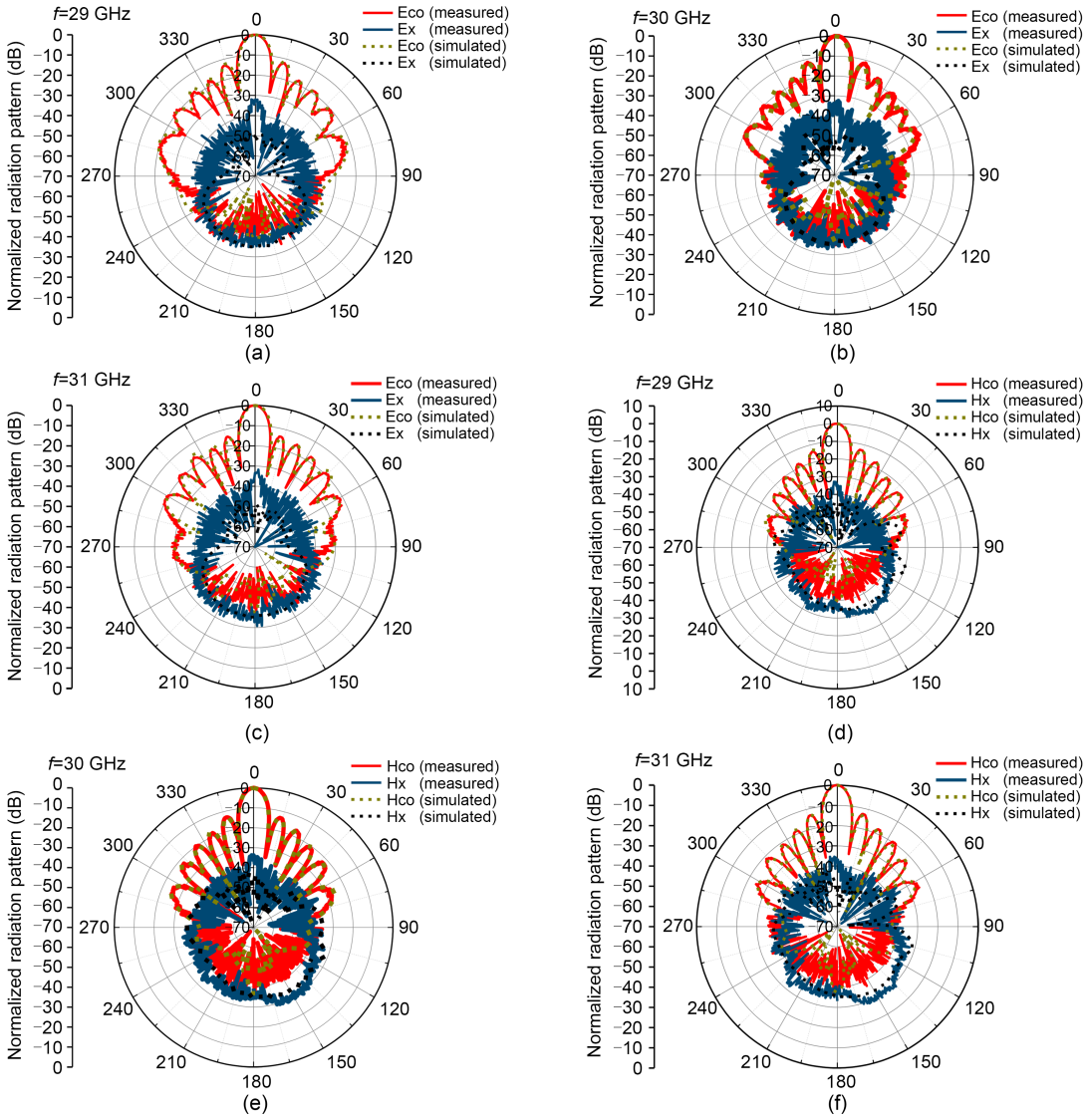

Fig. 13 Simulated and measured normalized radiation patterns of the shared-aperture array antenna at Ka-band: E-plane (*yoz* plane) at 29 GHz (a), 30 GHz (b), and 31 GHz (c); H-plane (*xoz* plane) at 29 GHz (d), 30 GHz (e), and 31 GHz (f)

agreement with the simulated ones, and a low cross-polarization level below −30 dB is achieved for the proposed array antenna. Note that the proposed antenna can provide only linear polarization. To support millimeter-wave low Earth orbit satellite communication, circular polarization is required for the antenna. To this end, a cross-radiation slot can be adopted in the design instead of two types of radiation slots in the proposed antenna, and can be used to generate circular polarization using a 90° phase shifting stripline feeding network and the forked stripline feeding SIW cavity for the K- and Ka-band applications, respectively.

Table 1 shows the comparison between the proposed and relative millimeter-wave shared-aperture array antennas in the literature. Generally, the proposed antenna has good performance in terms of bandwidth, port isolation, and aperture size. Note that the profile of the antenna is only 1.91 mm, which is suitable for planar applications.

4 Conclusions

A compact 8×8 dual-polarized shared-aperture array antenna is presented in this paper. A hybrid slot that combines the butterfly-shaped transverse slots and parallel slot pairs was designed for K- and Ka-band radiations, independently. Different radiation

Table 1 Comparisons between the proposed and relative millimeter-wave shared-aperture array antennas

Reference	Array scale	Center frequency (GHz)	FBW (%)	Max gain (dBi)	Isolation (dB)	Size ($\lambda_u \times \lambda_u$)
Ferrando-Rocher et al. (2019)	8×8	20/30	10/6	26/29.5	80/50	9.35×9.35
Ding and Cheng (2019)	4×4	16/34.7	12.5/4.1	13.2/17.2	70/28	3.2×1.7
Guo et al. (2021)	8×8	19/29	14.7/20.7	21.4/22	60/50	9.86×8.7
This work	8×8	19/30	7.73/20	18.5/20.02	60/44	5.8×5.8

λ_u is the wavelength of the center frequency of the higher band. FBW is the fractional bandwidth. The numbers before and after "/" represent the corresponding performance of the two antennas with different center frequencies

modes were used for the K- and Ka-band radiations, along with orthogonal polarizations. Consequently, high band isolation was achieved. The designed prototype was fabricated using PCB technology, and the measurement results were in good agreement with the simulation ones. The proposed antenna has the advantages of dual-band operation capability, high band isolation, planar form, and small size, and has great potential to reduce the size of wireless systems.

Contributors

Zhangcheng HAO proposed the idea. Yuyan CAO designed and measured the antenna, processed the experimental data, and drafted the paper. Zijun GUO helped design the antenna and organize the paper. All the authors revised and finalized the paper.

Compliance with ethics guidelines

Yuyan CAO, Zijun GUO, and Zhangcheng HAO declare that they have no conflict of interest.

References

Cheng YJ, Wang J, Liu XL, 2017. 94 GHz substrate integrated waveguide dual-circular-polarization shared-aperture parallel-plate long-slot array antenna with low sidelobe level. *IEEE Trans Antenn Propag*, 65(11):5855-5861. https://doi.org/10.1109/TAP.2017.2754423

Ding YR, Cheng YJ, 2019. Ku/Ka dual-band dual-polarized shared-aperture beam-scanning antenna array with high isolation. *IEEE Trans Antenn Propag*, 67(4):2413-2422. https://doi.org/10.1109/TAP.2019.2894270

Ferrando-Rocher M, Herranz-Herruzo JI, Valero-Nogueira A, et al., 2019. Full-metal K-Ka dual-band shared-aperture array antenna fed by combined ridge-groove gap waveguide. *IEEE Antenn Wirel Propag Lett*, 18(7):1463-1467. https://doi.org/10.1109/LAWP.2019.2919928

Guo ZJ, Hao ZC, Yin HY, et al., 2021. Planar shared-aperture array antenna with a high isolation for millimeter-wave low Earth orbit satellite communication system. *IEEE Trans Antenn Propag*, 69(11):7582-7592. https://doi.org/10.1109/TAP.2021.3083786

Ho KMJ, Rebeiz GM, 2014. Dual-band circularly-polarized microstrip antenna for Ku/Ka band statellite communication arrays. Proc IEEE Antennas and Propagation Society Int Symp, p.1831-1832. https://doi.org/10.1109/APS.2014.6905242

Hong W, Yue GR, Ge XH, et al., 2021. High-throughput millimeter-wave wireless communications. *Front Inform Technol Electron Eng*, 22(4):437-440. https://doi.org/10.1631/FITEE.2120000

Li D, Xu JG, Zhang B, et al., 2015. GCPW to stripline vertical transition for K-band applications in LTCC. Asia-Pacific Microwave Conference, p.1-3. https://doi.org/10.1109/APMC.2015.7413526

Luo GQ, Hu ZF, Dong LX, et al., 2008. Planar slot antenna backed by substrate integrated waveguide cavity. *IEEE Antenn Wirel Propag Lett*, 7:236-239. https://doi.org/10.1109/LAWP.2008.923023

Mao CX, Gao S, Wang Y, et al., 2017a. A shared-aperture dual-band dual-polarized filtering-antenna-array with improved frequency response. *IEEE Trans Antenn Propag*, 65(4):1836-1844. https://doi.org/10.1109/TAP.2017.2670325

Mao CX, Gao S, Luo Q, et al., 2017b. Low-cost X/Ku/Ka-band dual-polarized array with shared aperture. *IEEE Trans Antenn Propag*, 65(7):3520-3527. https://doi.org/10.1109/TAP.2017.2700161

Mao CX, Gao S, Wang Y, et al., 2017c. Dual-band circularly polarized shared-aperture array for C-/X-band satellite communications. *IEEE Trans Antenn Propag*, 65(10):5171-5178. https://doi.org/10.1109/TAP.2017.2740981

Mukherjee S, 2017. Design of four-way substrate integrated coaxial line (SICL) power divider for K band applications. Proc IEEE MTT-S Int Microwave and RF Conf, p.1-4. https://doi.org/10.1109/IMaRC.2017.8449663

Naishadham K, Li RL, Yang L, et al., 2013. A shared-aperture dual-band planar array with self-similar printed folded dipoles. *IEEE Trans Antenn Propag*, 61(2):606-613. https://doi.org/10.1109/TAP.2012.2216491

Qi ZH, Li XP, Zhu H, 2021. Low-cost high-order-mode cavity backed slot array antenna using empty substrate integrated waveguide for the 5G n260 band. *Front Inform Technol Electron Eng*, 22(4):609-614. https://doi.org/10.1631/FITEE.2000503

Smolders AB, Mestrom RMC, Reniers ACF, et al., 2013. A shared aperture dual-frequency circularly polarized microstrip array antenna. *IEEE Antenn Wirel Propag Lett*, 12:

120-123. https://doi.org/10.1109/LAWP.2013.2242427

Tao MC, Wu YW, Hao ZC, 2021. Compact orthogonal multiple-beam antenna with shared aperture. *IEEE Antenn Wirel Propag Lett*, 20(6):873-877. https://doi.org/10.1109/LAWP.2021.3060771

Wang K, Liang XL, Zhu WR, et al., 2018. A dual-wideband dual-polarized aperture-shared patch antenna with high isolation. *IEEE Antenn Wirel Propag Lett*, 17(5):735-738. https://doi.org/10.1109/LAWP.2018.2812699

Xu J, Hong W, Jiang ZH, et al., 2020. Low-cost millimeter-wave circularly polarized planar integrated magneto-electric dipole and its arrays with low-profile feeding structures. *IEEE Antenn Wirel Propag Lett*, 19(8):1400-1404. https://doi.org/10.1109/LAWP.2020.3002343

Xu LM, Wan YT, Yu D, 2019. Research of dual-band dual circularly polarized wide-angle scanning phased array. Proc IEEE 2nd Int Conf on Automation, Electronics and Electrical Engineering, p.22-25. https://doi.org/10.1109/AUTEEE48671.2019.9033428

Zhang JD, Wu W, Fang DG, 2016. Dual-band and dual-circularly polarized shared-aperture array antennas with single-layer substrate. *IEEE Trans Antenn Propag*, 64(1): 109-116. https://doi.org/10.1109/TAP.2015.2501847

Zhang JF, Cheng YJ, Ding YR, et al., 2019. A dual-band shared-aperture antenna with large frequency ratio, high aperture reuse efficiency, and high channel isolation. *IEEE Trans Antenn Propag*, 67(2):853-860. https://doi.org/10.1109/TAP.2018.2882697

Zhang JF, Cheng YJ, Ding YR, 2020. An S- and V-band dual-polarized antenna based on dual-degenerate-mode feeder for large frequency ratio shared-aperture wireless applications. *IEEE Trans Antenn Propag*, 68(12):8127-8132. https://doi.org/10.1109/TAP.2020.2983769

Zhang Y, Chen ZN, Qing XM, et al., 2011. Wideband millimeter-wave substrate integrated waveguide slotted narrow-wall fed cavity antennas. *IEEE Trans Antenn Propag*, 59(5):1488-1496. https://doi.org/10.1109/TAP.2011.2123055

Zhao HD, Wang ZX, Meng HF, 2015. A design of E/Ka dual-band patch antenna array with shared aperture. Proc Asia-Pacific Microwave Conf, p.1-3. https://doi.org/10.1109/APMC.2015.7413001

Zhou GN, Sun BH, Liang QY, et al., 2021. Triband dual-polarized shared-aperture antenna for 2G/3G/4G/5G base station applications. *IEEE Trans Antenn Propag*, 69(1): 97-108. https://doi.org/10.1109/TAP.2020.3016406